Inorganic Chemistry
Cite This: Inorg. Chem. XXXX, XXX, XXX−XXX
Article
pubs.acs.org/IC

Structural Diversity of Coordination Polymers Based on a Heterotopic Ligand: Cu(II)-Carboxylate vs Cu(I)-Thiolate

Oleksandra Veselska,[†] Liwen Cai,[†,‡] Darjan Podbevšek,[§] Gilles Ledoux,[§] Nathalie Guillou,[∥] Guillaume Pilet,[‡] Alexandra Fateeva,*[,‡] and Aude Demessence*[,†]

[†]Univ Lyon, Université Claude Bernard Lyon 1, Institut de Recherches sur la Catalyse et l'Environnement de Lyon (IRCELYON), UMR 5256 CNRS, Villeurbanne, France

[‡]Univ Lyon, Université Claude Bernard Lyon 1, Laboratoire des Multimatériaux et Interfaces (LMI), UMR CNRS 5615, Villeurbanne, France

[§]Univ Lyon, Université Claude Bernard Lyon 1, Institut Lumière Matière (ILM), UMR CNRS 5306, Villeurbanne, France

[∥]Université de Versailles Saint-Quentin-en Yvelines, Université Paris-Saclay, Institut Lavoisier de Versailles (ILV), UMR CNRS 8180, Versailles, France

Supporting Information

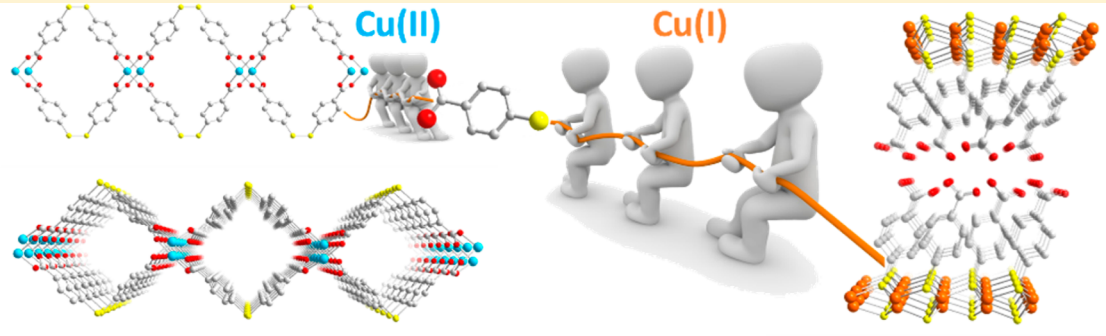

ABSTRACT: Two copper(II)-carboxylate disulfide coordination polymers $[Cu_2((O_2CPhS)_2)_2(H_2O)_2]_n$ (**1**, **2**) and one copper(I)-thiolate coordination polymer $[Cu(p\text{-}SPhCO_2H)]_n$ (**3**) have been synthesized using either the 4-mercaptobenzoic acid ($HSPhCO_2H$) or the 4,4′-dithiodibenzoic acid ($(SPhCO_2H)_2$) as ligand. These three compounds were characterized by X-ray diffraction, IR, and thermogravimetric analyses. Compounds **1** and **2** are polymorphs with the presence, for both, of dinuclear paddle-wheel copper(II)-carboxylates. In **1**, the adjacent dimeric Cu_2 units are linked by two $(O_2CPhS)_2$ ligands generating a cyclic loop chain, and in **2**, each pair of Cu (II) atoms is linked by four ligands to create 2D networks, that are 2-fold interpenetrated. Compound **3** presents a lamellar structure, with an exceptional thermal and chemical stability, and exhibits intrinsic multiple emission between 485 and 660 nm. The different intensities of these bands generate a cyclic luminescence thermochromism from yellow to green to yellow.

INTRODUCTION

The design and synthesis of coordination polymers have achieved considerable progress over the past decade, in order to control the molecular organization in the solid state and generate hybrid materials with novel topological structures and promising properties.[1] One approach to reach (multi)-functional materials is to use heterotopic ligands to induce heterometallic or mixed valency materials that will exhibit their own properties and potential applications in the fields of gas storage, magnetism, optical properties, or catalysis.[2] Thus, the organic ligands play a crucial role for the construction of coordination networks, and their most important parameters are the coordinating function, number and mode, the flexibility/rigidity, and the geometry. Among various coordinating groups, carboxylic acids have been extensively used, mainly due to their ability to generate iono-covalent bonding between the carboxylate and the metallic ion and their diverse coordination modes. HKUST-1 (copper benzene-1,3,5-tricarboxylate) is an archetype MOF with a highly porous network based on Cu(II)-carboxylate paddle wheel units.[3] Nevertheless, one of the drawbacks of most Cu(II)-carboxylate MOFs is their lack of stability in water or air due to the relatively weak interaction between the metal and the carboxylate.[4] Among the diverse coordinating functions, thiolates are largely used in nanotechnology to synthesize, functionalize, and protect metallic nanoparticles, as they display strong affinity toward coinage metals through soft−soft interactions. In copper coordination chemistry, a limited number of nine structures of neutral Cu(I)-thiolate coordination polymers, $[Cu(SR)]_n$,

Received: December 12, 2017

DOI: 10.1021/acs.inorgchem.7b03090
Inorg. Chem. XXXX, XXX, XXX−XXX

have been reported so far.[5] Copper thiolates with SR = SMe,[6] *p*-SPhX (X = H, Me, OMe, NO_2),[7] and S(di)adamantane[8] form chain-like coordination polymers, while when X = OH[9] and CO_2Me[10] the compounds display layered structures. Some of these emerging $[Cu(SR)]_n$ coordination polymers exhibit electrical conductivity through 1D structures,[8] or 2D sheets,[11] and some are photoluminescent with unusual intrinsic triple emission, being of a great potential as ratiometric temperature sensing.[10] These limited but promising studies on copper thiolates highlight their high potential as multifunctional materials.

In addition, due to the rich redox chemistry of thiols, oxidative formation or reductive cleavage of the disulfide bonds can be induced depending on the reaction medium. Numerous coordination polymers have been prepared with bidentate disulfide-based ligands in different basic or acidic media at room temperature or under solvothermal conditions.[12] The diversity of the structures is due to the flexibility/rotation of the S−S bond. *In situ* cleavage of the S−S bond has already been observed under solvothermal conditions, implying the formation of coordination polymers with either coordinated thiolate, sulfinate, or sulfonate functionalities.[12a,f,13] Synthesis of coordination polymers with *in situ* S−S formation from a thiol ligand has also been reported.[14] Finally, a same coordination polymer could also be obtained by either a direct assembly synthetic route with a disulfide or with an *in situ* S−S bond formation from the thiol parent.[14c] Interestingly, a simultaneous Cu(II) to Cu(I) reduction and S−S reductive cleavage of 4,4′-dipyridyl disulfide was reported to happen under solvothermal conditions.[13g]

In this work, we aimed to rationalize and understand the coordination of the thiolate to Cu(I) and of the carboxylate moiety to Cu(II) for closely related organic ligands. The heterotopic 4-mercaptobenzoic acid ($HSPhCO_2H$) and its oxidized dimeric form, the 4,4′-dithiodibenzoic acid ($(SPhCO_2H)_2$), are studied to evaluate the impact of the reaction conditions on the redox chemistry of thiol/disulfide functions, meaning formation/breaking of S−S bonds and the coordination of thiolate and carboxylates with copper. Two polymorphic copper(II)-carboxylate disulfide coordination polymers $[Cu_2((O_2CPhS)_2)_2(H_2O)_2]_n$, **1** and **2**, and one lamellar copper(I)-thiolate compound $[Cu(p\text{-}SPhCO_2H)]_n$, **3**, have been successfully synthesized starting with either the oxidant or the reductive forms of the ligand (Scheme 1). In-depth structural characterizations, chemical and thermal stability studies, and photoluminescence properties for **3** are discussed.

Scheme 1. Synthetic Routes of Compounds 1−3

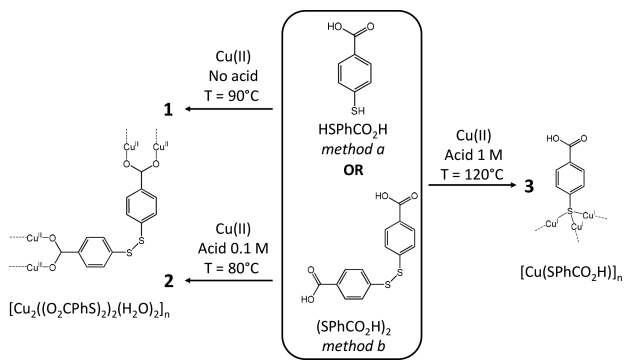

RESULTS AND DISCUSSION

Synthesis. In this study, we used systematically both ligands under the same reaction conditions to evaluate their reactivity: methods a and b are respectively assigned for the synthesis starting from the thiol-based ligand $HSPhCO_2H$ or the disulfide-based ligand $(SPhCO_2H)_2$ (see syntheses in the Supporting Information). When either of these two ligands is reacted with Cu(II) in DMF at 90 °C in a closed vessel, the same compound **1** is obtained by methods a and b, as evidenced from PXRD data (Scheme 1 and Figure 1). When

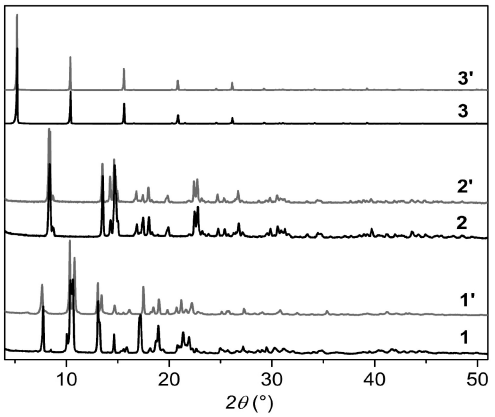

Figure 1. Powder X-ray diagrams of compounds **1**−**3** and **1′**−**3′** obtained by method a and b, respectively.

the reaction conditions are slightly changed by adding a 0.1 M solution of a strong acid and lowering the temperature to 80 °C, a second compound **2** is isolated either by method a or b (Scheme 1 and Figure 1). Compounds **1** and **2** are polymorphs, with the formula, $[Cu_2((O_2CPhS)_2)_2(H_2O)_2]_n$, based on the same Cu(II)-carboxylate paddle wheel motif. This observation points out that the addition of an acid plays here a crucial role on the structure but not on the connectivity; this will be further discussed in the structural description part. Nevertheless, the synthesis of pure **1** and **2** is highly dependent on the type of metallic salt and the acid, as reported in the Supporting Information, and changing the conditions will afford a mixture of compounds, including other polymorphs impossible to isolate as a pure phase. Finally, when harsher conditions are employed, 120 °C with the addition of 1 M acid solution, S−S bond cleavage and Cu(II) to Cu(I) reduction are observed for both methods a and b (Scheme 1 and Figure 1). The formation of the Cu(I)-thiolate, $[Cu(p\text{-}SPhCO_2H)]_n$ (**3**), is less sensitive to the type of precursors and can be obtained with either copper nitrate or copper chloride, with 0.1 or 1 M nitric or hydrochloric acid and even at 80 °C (Scheme 1 and the Supporting Information). High yield and the best crystallinity were obtained at 120 °C with 1 M acid. In **3**, the coordination proceeds through the thiolates to Cu(I) and the carboxylic acids remain protonated. The formation of a coordination polymer involving *in situ* reduction of Cu(II) to Cu(I) coupled with the reductive cleavage of the S−S bond has also been observed with the 4,4′-dithiodipyridine under solvothermal conditions.[13g]

Thus, under mild conditions of temperature (80−90 °C) and with or without a small amount of acid, an oxidative medium is favored and leads to the formation or conservation of S−S bonds and coordination of the carboxylates with Cu(II). The formation of compounds **1** and **2** from method a is explained

DOI: 10.1021/acs.inorgchem.7b03090
Inorg. Chem. XXXX, XXX, XXX−XXX

by the redox chemistry of Cu(II) and mercaptans that is known as the "Perco" process to sweeten gasoline and to convert the foul smelling thiols into less offensive disulfides (Scheme 2a).[15]

Scheme 2. Reaction Mechanisms Involved in the Formation (a) of 1 and 2 and (b) of 3[a]

a. Perco sweetening process:

Step 1: $2\,HSR + 2\,Cu(II) \rightarrow RSSR + 2\,Cu(I) + 2\,H^+$

Step 2: $2\,Cu(I) + \tfrac{1}{2}\,O_2 + 2\,H^+ \rightarrow 2\,Cu(II) + H_2O$

Net reaction: $2\,HSR + \tfrac{1}{2}\,O_2 \rightarrow RSSR + H_2O$

b. Redox reaction:

$2\,HSR + Cu(II) \rightarrow Cu(I)SR + \tfrac{1}{2}\,RSSR + 2\,H^+$

[a]HSR and RSSR are for thiol and disulfide ligands.

In that case, the Cu(II) is not consumed in the process because the dioxygen from the air reoxidizes Cu(I) back to Cu(II). When more extreme conditions of temperature (120 °C) and acidity (1 M) are employed, the formation of copper(I)-thiolate is favored. The effect of Cu(II) Lewis acidity on S−S polarization may be involved in the S−S breaking,[16] and then, the redox reaction between Cu(II) and the thiols results in the formation of **3**. This study shows that the coordination of carboxylates or thiolates is controlled by the synthesis medium rather than by the redox state of the sulfur atoms.

Structural Description. **1** crystallizes in the monoclinic centrosymetrical *C*2/*m* space group and displays a 1D framework with the asymmetric unit consisting of one Cu(II) atom lying in the mirror plane and one-half of a ligand unit $(O_2CPhS)^-$ (Figure 2 and Table S1). The metal center environment can be described as a distorted square-pyramidal geometry within each Cu(II) being coordinated in the equatorial plane to four oxygen atoms, each of these later belonging to four different carboxylate ligands. The coordination sphere around the 3d metal is completed by one oxygen atom from a water molecule in the axial position. Cu−O bond lengths are equal to 1.958(4) and 1.972(6) Å for the carboxylate oxygen atoms and are shorter than the one (2.139(6) Å) involving the coordinated water molecule (Table S2). Two adjacent Cu(II) atoms are bridged by four carboxylate units from four ligand molecules giving rise to a paddle-wheel-shaped geometry exhibiting a short Cu···Cu distance (2.647(2) Å, Figure 2a and Table S2). $[(O_2CPhS)_2]^{2-}$ ligands adopt a V-shaped conformation illustrated by a C−S−S disulfide bond angle of 105.92 (2)° and a C−S−S−C torsion angle of 73.64(2)°. Each ligand bridges two dimeric $\{Cu_2\}$ units, giving rise to a 1D cyclic loop chain (Figure 2a and b) running along the [001] direction of the unit-cell. A view along the *c*-axis of the unit-cell (Figure 2c) clearly shows that there is no connection between the metal−organic chains. The distance between the chains is 3.682(3) Å along the *b* axis (distance between disulfide bonds of two chains).

Compound **2** crystallizes in the monoclinic centrosymetrical *C*2/*c* space group and displays a 2D framework. The asymmetric unit here is made up of one Cu(II) atom and one $[(O_2CPhS)_2]^{2-}$ ligand (Figure 3 and Table S1). Each Cu(II) atom, located in a ML_5 {O5} square-base pyramidal environment, is coordinated in the same way as for **1**, by four oxygen atoms from four carboxylate ligands in the equatorial plane and one oxygen atom from a water molecule which occupies the axial position. The Cu−O bond lengths range from 1.951(4) to 1.983(4) Å in the equatorial plane and are shorter than the one (2.150(4) Å) located in the axial position (Table S2). Comparably to what was observed for **1**, Cu(II) atoms are arranged in dimeric paddle wheel units by bidentate bridging carboxylate functions with a Cu···Cu distance of 2.609(1) Å (Figure 3a and Table S2). The $[(O_2CPhS)_2]^{2-}$ adopts a V-shaped conformation with a C−S−S angle identical to the precedent one but with a different C−S−S−C torsion angle (91.10(3)°). Each ligand bridges two dimeric Cu paddle wheel units, and each dimer is connected to four ligands; this gives rise to a 2D polymer (Figure 3b and c), and two identical 2D networks are interpenetrated with each other to result in a 2-fold interpenetrated framework (Figure S1).

In these two compounds, the inorganic paddle wheel units display the same coordination environments but the overall framework arrangements greatly differ between **1** and **2**. Compound **1** crystallizes in the *C*2/*m* space group with the mirror plane (0,1,0) passing through the two Cu(II) atoms of the paddle wheel. This particular situation imposes the metallocyclic motif for the ligand arrangement, generating the 1D looplike chain. In this structure, all of the Cu(II) dimers are aligned in (a,c) planes. In the case of compound **2**, the Cu(II) dimers are no longer aligned, and if considering two dimers bridged by one ligand molecule, a torsion angle of 59.87(3)° appears between the directions of each Cu···Cu dimer. This

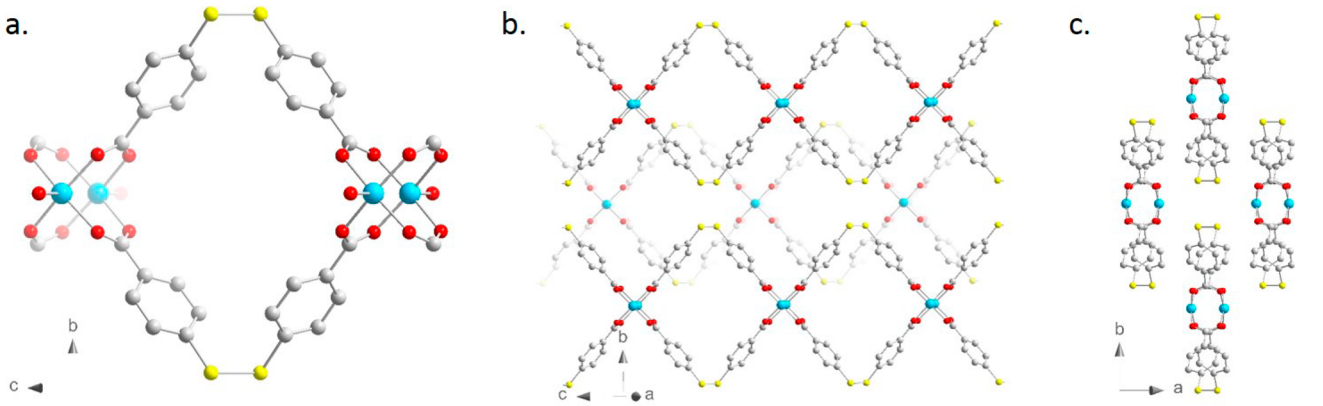

Figure 2. (a) Local coordination environment of the Cu(II) ion in compound **1**. (b) View of the 1D coordination polymeric ribbon in compound **1** along the *c* axis. (c) Projection of the 1D coordination polymer **1** on the *c* axis. Blue, Cu(II); yellow, S; red, O; gray, C. Hydrogen atoms and water molecules are omitted for clarity.

DOI: 10.1021/acs.inorgchem.7b03090
Inorg. Chem. XXXX, XXX, XXX−XXX

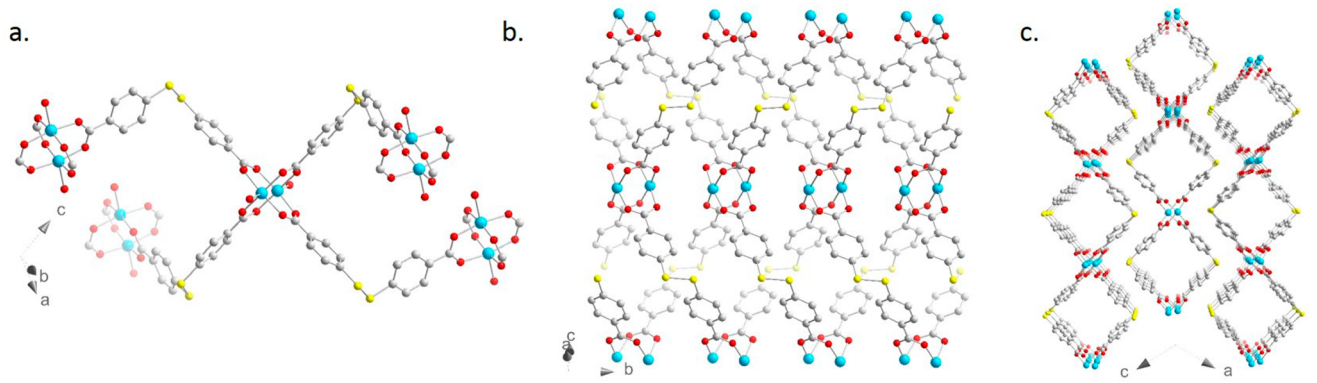

Figure 3. (a) Local coordination environment of the Cu(II) ion in compound **2**. (b) View of 2D coordination polymer in compound **2** and (c) central projection of **2** along the *b* axis. Blue, Cu(II); yellow, S; red, O; gray, C. Hydrogen atoms and water molecules are omitted for clarity.

way, the polymeric network expands in two directions, generating a 2D network. The disulfide S−S bond in the $[(O_2CPhS)_2]^{2-}$ ligand can rotate freely, hence bringing flexibility to the possible conformations. In compounds **1** and **2**, the C−S−S−C torsion angles are quite different: 73.64(2)° for **1** that allows a metallocyclic motif to be generated and 91.10(3)° for **2** where the ligand has a more corrugated nature that favors the formation of the 2D interpenetrating structure (Figure 4). These results show that the flexibility of the

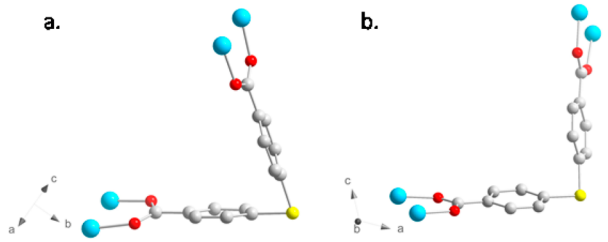

Figure 4. Coordination modes of the $[(O_2CPhS)_2]^{2-}$ ligand in **1** (a) and **2** (b) with a projection along the −S−S− axis. Blue, Cu(II); yellow, S; red, O; gray, C. Hydrogen atoms are omitted for clarity.

disulfide ligand $[(O_2CPhS)_2]^{2-}$ can lead to a structural diversity when keeping the inorganic unit unchanged. Here, linear metallocyclic motifs are obtained in compound **1** and interpenetrating 2D structure in compound **2**. However, the particular factors ruling the particular structure formation with the flexible S−S spacer of $[(O_2CPhS)_2]^{2-}$ ligand have not been well explored so far and more work is needed to elucidate them.

Compound **3** crystallizes in the orthorhombic centrosymetrical *Pbca* space group (Figure 5 and Table S1). Its formula is $[Cu(p\text{-}SPhCO_2H)]_n$, and its refined structural model displays a layered structure, related to the only two other 2D Cu(I) thiolate polymers reported to date, $[Cu(p\text{-}SPhOH)]_n$[9] and $[Cu(p\text{-}SPhCO_2Me)]_n$.[10] The Cu(I) atoms are in trigonal geometry and are linked to three sulfur atoms from three $(p\text{-}SPhCO_2H)^-$ ligands. Each sulfur bridges three Cu(I) atoms, generating $\{Cu_3S_3\}$ distorted hexagons that lie in layers propagating in the (ab) plane (Figure 5a and b). The Cu−S distances are 2.243(3), 2.290(2), and 2.302(3) Å, and the S−Cu−S angles are 104.12(7), 125.96(11), and 129.82(10)° (Table S2). The shortest Cu···Cu distance is 3.030(2) Å which is slightly shorter to those which were reported before in similar structures but still greater than the sum of van der Waals radii (2.80 Å). Therefore, no cuprophilic interactions are expected in compound **3**. In between the Cu−S layers lies the organic part, and the presence of carboxylic acids generates interactions between the layers through dimeric hydrogen bonds (Figure 5c and d). The presence of these weak interactions possibly favors the formation of the distorted $\{Cu_3S_3\}$ hexagons compared to

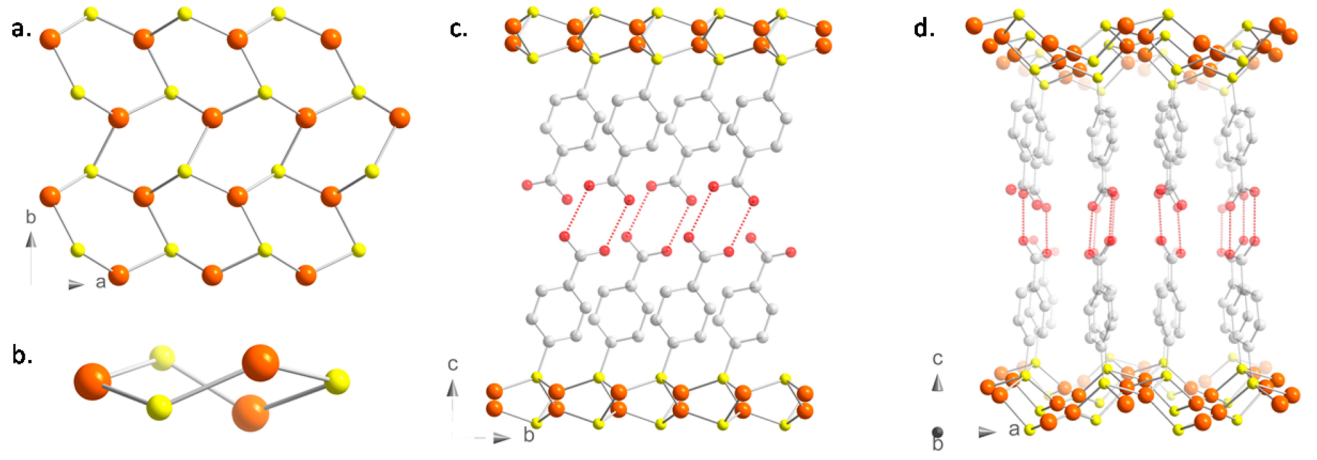

Figure 5. Structure of **3**: (a) representation of the Cu_3S_3 network on the (ab) plane, (b) view of a Cu_3S_3 cycle, (c and d) projections of the lamellar structure on the (bc) and (ac) planes, respectively. Orange, Cu(I); yellow, S; gray, C. Red dotted lines show the hydrogen bonds. Hydrogen atoms are omitted for clarity.

DOI: 10.1021/acs.inorgchem.7b03090
Inorg. Chem. XXXX, XXX, XXX−XXX

the half-chair observed for the analogue with the ester functions $[Cu(p\text{-}SPhCO_2Me)]_n$.[10]

Characterizations. The phase purity of **1**−**3** was confirmed by powder X-ray diffraction (PXRD), scanning electron microscopy (SEM), Fourier transform Infrared spectroscopy (FTIR), and thermogravimetric analysis (TGA) carried out under air. The experimental PXRD patterns of **1**−**3** are consistent with the calculated diagrams (Figure S2), and the Rietveld refinement of **3** provides excellent factors of merit (Figure S3), demonstrating an effective method to obtain these compounds with extremely high purity and crystallinity. SEM images reveal that the crystallites of each phase display their own particular shape; **1** has a cuboid form, **2** has an elongated stick shape, and **3** is constituted of plates characteristic of lamellar compounds (Figure S4). More importantly, only one type of crystal morphology is observed for each solid, confirming the purity. Both Cu(II)-based compounds, **1** and **2**, show the same FTIR spectra (Figure S5). Compared to the noncoordinated ligands, the disappearance of the large band at 2500−3100 cm^{-1}, which is attributed to −OH stretching of carboxylic acid, is in good accordance with the coordination of the carboxylate to Cu(II). In addition, the asymmetric and symmetric vibrations of the carboxylates at 1590 and 1400 cm^{-1} are typical of a bridging coordination mode (Figure S6). The band at 1680 cm^{-1} is attributed to the vibration of the CO of the DMF that was used as a solvent. The FTIR spectrum of **3** exhibits the same large and intense band at 2500−3100 cm^{-1} as the starting ligands, showing that the carboxylic acids interact together through hydrogen bonds (Figure S5). The presence of the uncoordinated carboxylic acids is also confirmed by the antisymmetric vibration of COO at 1680 cm^{-1} (Figure S6).

The TGA profiles of **1** and **2** under air are quasi similar, and solvent molecules are removed up to 200 °C with a total weight loss of 12.7%, pointing out that the free and coordinated water and DMF molecules are removed (Figure S7). The compounds **1** and **2** start to decompose at 320 °C and **3** at 290 °C under air flow. The remaining CuO at 800 °C for **1** and **2** of 22.9% (calc. 21.6%) and for **3** of 37.1% (calc. 36.7%) are close to the expected values. The slight difference between calculated and experimental values can be explained by the formation of $Cu_2O(SO_4)$ along with CuO. Indeed, the three compounds exhibit a first plateau at 400 °C which corresponds to a majority of $Cu_3(OH)_4(SO_4)$ with a small amount of $Cu(SO_4)(H_2O)_5$ and a second one at 700 °C which is mainly CuO with a minor quantity of $Cu_2O(SO_4)$ (Figure S8). Thus, when the TGA is carried out under nitrogen flow, **2** exhibits the same temperature of decomposition, while **3** remains more stable and starts to decompose at 350 °C (Figure S7). The final product obtained at 800 °C under nitrogen has been analyzed by PXRD and proves the presence of chalcocite (Cu_2S), which is more crystalline in **3** than in **2**, plus an amorphous phase in both compounds (Figure S9).

Thermal and Chemical Stability. Due to the potential porosity of compound **2** and the luminescent properties of **3**, their thermal and chemical stability were studied (see the Supporting Information for experimental conditions). First, when the solid **2** is heated under air at 150 °C for 12 h, the PXRD shows a phase change with the appearance of new peaks; nevertheless, no decomposition is observed (Figure S10). SEM images show that crystals of **2** are sliced upon the heat treatment (Figure S11). Second, when the solid **2** is introduced in a Soxhlet with several cycles of MeOH for 12 h, its structure remains unchanged, pointing out its chemical stability in hot MeOH (Figure S10). The TGA curve shows the presence of 5% MeOH that is removed at 100 °C (Figure S12). In addition, **2** is still stable under the reducing conditions of $NaBH_4$ for 3 h at room temperature; no S−S bond breaking is observed, and the PXRD pattern remains unchanged (Figure S10). FT-IR of the solids heated at 150 °C and after MeOH Soxhlet extraction shows the disappearance of the CO vibration of the DMF at 1680 cm^{-1}, meaning the total removal of the solvent molecules (Figure S13). Nevertheless, the N_2 adsorption at 77 K on **2** after activation does not show any permanent porosity.

The solid **3** exhibits an exceptional thermal and chemical stability. Indeed, after heating at 250 °C under air for 1 h, the PXRD reveals no changes (Figure S14). When dispersed in boiling water for 24 h, the solid remains crystallographically intact (Figure S14). Even better, under acidic conditions, the powder is still highly crystalline after 24 h stirring in a 1 M HCl solution, as shown by the PXRD (Figure S15). In basic media, no structural change is observed from the PXRD data when the solid is dispersed for 24 h in 0.1 M NaOH solution (Figure S15). However, in a more basic solution of 1 M NaOH, the reflections of **3** disappear for a new lamellar phase with a shift of the first peak from 5.20 to 4.89° (2θ). This observation points out a structural change to a different lamellar compound with a longer interlamellar distance of 1.80 nm (instead of 1.70 nm) that most probably corresponds to the insertion of sodium cation to form $[Cu(p\text{-}SPhCO_2Na)]_n$. The saponification of the carboxylic acids is also confirmed by FT-IR that shows the disappearance of the large band at 2500−3100 cm^{-1} coming from the hydrogen bonds and the shift of the $\nu_{as}(COO)$ at 1680 cm^{-1} (Figure S16). Nevertheless, the formation of aligned wires of a couple of hundred nanometers of thickness on the SEM images of $[Cu(p\text{-}SPhCO_2Na)]_n$, points out that the topology of Cu−S may be different from **3**, and that a dissolution-recrystallization mechanism may had happened (Figure S17). Finally, the solid **3** is still stable when it is stirred for 24 h in an oxidant media with 1% H_2O_2 but starts to decompose in strong oxidizing solution of 10% H_2O_2 and the formation of crystalline disulfide ligand, $(SPhCO_2H)_2$, is observed (Figure S18). Consequently, the copper(I)-thiolate coordination polymer is stable up to 250 °C in air and under acidic and basic conditions as well as in mild oxidant medium. The thermal and chemical stability observations agree with the stronger nature of the Cu(I)-thiolate coordination bonds when compared to the Cu(II)-carboxylate one.

Photophysical properties of 3. Cu(I)-thiolates have been attracting considerable attention owing to their interesting photochemical properties.[17] With respect to the luminescence mechanism, the coordination of Cu(I) with thiolate ligands usually leads to ligand-to-metal charge transfer (LMCT) and/or ligand-to-metal−metal charge transfer (LMMCT), which can generate radiative relaxation via a metal-centered triplet state.[10,13g,18] The UV−vis absorption spectrum of **3** shows an intense band with a maximum centered at 364 nm and a smaller one at 278 nm (Figure S19). The deduced optical bandgap of 2.79 eV is close to the one reported for the 1D and 2D $[Cu(SR)]_n$ analogues (2.2−2.9 eV).[5,10]

As depicted in Figure S20, **3** exhibits some luminescence thermochromism when irradiated under UV light in the solid state. It is light yellow from room temperature to 243 K, becomes green between 213 and 153 K, and is back to intense yellow from 123 to 93 K. Thus, the photoluminescence studies have been carried out in the solid state in the range from 93 to 293 K. Excitation vs emission is plotted at different temper-

DOI: 10.1021/acs.inorgchem.7b03090
Inorg. Chem. XXXX, XXX, XXX−XXX

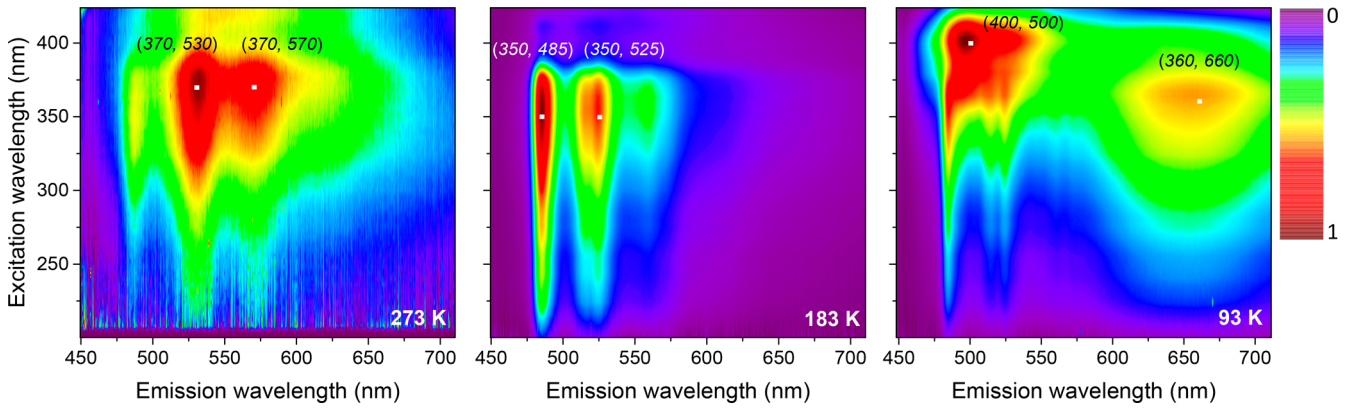

Figure 6. 2D maps of the emission and excitation spectra of **3**, $[Cu(p\text{-}SPhCO_2H)]_n$, carried out in the solid state at 273, 183, and 93 K. The white squares correspond to the coordinates (λ_{ex}, λ_{em}) in nm of the peaks.

atures on the 2D maps, and the coordinates (λ_{ex}, λ_{em}) in nm are used to describe the peak positions (Figures 6 and S21). From the 2D map at 273 K, **3** exhibits two peaks with the more intense one at (370, 530) and the second one at (370, 570). When the temperature decreases, a third peak appears at (350, 485) and is predominant from 213 to 123 K. Then, at 123 K, two other peaks appear at (400, 500) and (360, 660). Finally, those two peaks still increase when the temperature decreases and the one at (400, 500) becomes dominant. The presence of these four maxima of excitation from 350 to 400 nm and the five maxima of emission at 485, 500, 530, 570, and 660 nm can also be clearly seen on the 1D graphs of excitation and emission plotted at variable temperatures (Figures 7 and S22–S25). The

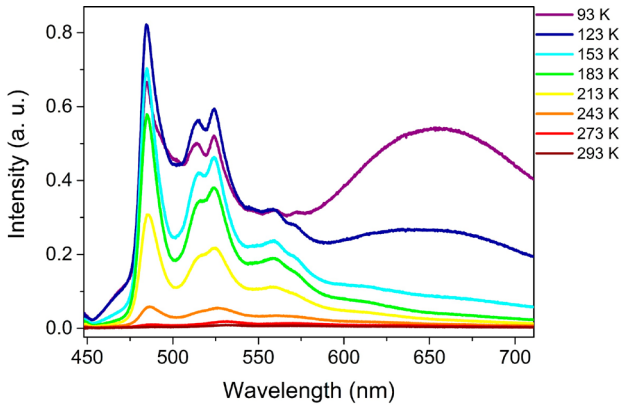

Figure 7. Emission spectra (λ_{ex} = 352 nm) of **3** in the solid state with the temperature.

temperature dependent CIE (Commision Internationale de l'Eclairage) chromaticity diagram (Figure 8) confirms the back and forth color change from yellow to green to yellow from 293 to 93 K, which is consistent with the changing intensities ratio of the multiple bands. To get more insight into the photophysical processes involved in **3** with the temperature, single crystal XRD analysis has been carried out at 120 K. When lowering the temperature, the space group of **3** is identical and the reduction of the cell volume of 0.55% from 293 to 120 K can be considered as negligible (Tables S1 and S2). Hence, the luminescence thermochromism of **3** is not directly correlated to some structural changes, as has been observed in some Cu(I) analogues.[19] The lifetime decay measurements carried out with λ_{ex} = 379 nm show that at 273

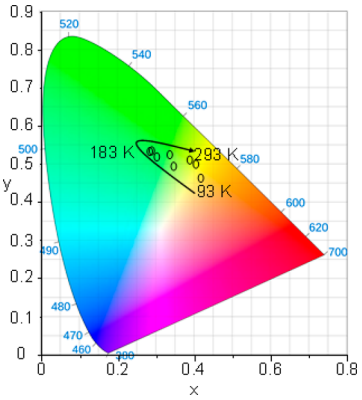

Figure 8. CIE chromaticity diagram showing the temperature-dependent luminescence color change of **3** in the 93–293 K temperature range (λ_{ex} = 352 nm).

K the emission lifetime has four contributions between 1 and 764 μs and at 93 K this lifetime increases with the contributions between 44 μs and 9.2 ms (Figure S26, Table S3). These long radiative lifetimes, in the microsecond and even millisecond ranges, are characteristic of triplet states and phosphorescent processes. From these different observations, the vibronic structure of the emission between 485 and 570 nm can be attributed to the aromatic thiolate as intraligand or ligand-to-ligand charge transfer ^{3}IL/LLCT involving $\pi \rightarrow \pi^*$ transitions. Indeed, when compared to the photoemission of the noncoordinated *p*-mercaptobenzoic acid, which exhibits a single emission band centered around 530 nm in the same range of temperature,[20] the apparition of the vibronic structure can be due to the rigidity of the ligand when coordinated to the metal or to the perturbation of a charge transfer due to the metal. The emission band at low energy, 660 nm, originates most probably from the triplet states of ligand-to-metal (^{3}LMCT) and/or metal-to-ligand charge-transfer transitions (^{3}MLCT), mixed with metal-centered (ds/dp) states. Hence, the luminescence thermochromism of **3** is a subtle equilibrium between ligand-centered (at high energy) and metal-centered (at low energy) charge transfers and the diminution of the nonradiative decays when the temperature decreases.[21] More detailed spectroscopic and theoretical studies need to be pursued to fully explain the origin of the bands. Two comparisons of the photoluminescence properties of Cu(I)-thiolates can be made with **3**: (i) the analogue $[Cu(p\text{-}SPhCO_2Me)]_n$[10] exhibits intense luminescence thermochrom-

DOI: 10.1021/acs.inorgchem.7b03090
Inorg. Chem. XXXX, XXX, XXX–XXX

ism with three well-separated emission bands at 460, 560, and 740 nm and emission up to 500 K, associated with a similar Cu_3S_3 lamellar structure, and (ii) [Cu(I)(pyridine-4-thiolate)]$_3$, made of interconnected clusters, is a green phosphor, with a single emission band centered at 560 nm.[13g] These comparisons point out that the origin of the multiple emission, the ratio and position of the bands, are a subtle combination of rigidity of the network induced by the hydrogen bonds, the π-stacking, the bond distances, and the function of the ligand. In fact, the photoluminescence of compound **3** presents more similarities with the lamellar compound, $[Au(p\text{-}SPhCO_2H)]_n$,[20] meaning the importance of the ligand in the photophysical properties. Thus, the MOCs are coordination polymers with a rich potential in terms of tuning the structures and the properties.[5]

CONCLUSIONS

In summary, we demonstrate the successful syntheses of three new coordination polymers, two copper(II)-carboxylate disulfide compounds **1** and **2**, $[Cu_2((O_2CPhS)_2)_2(H_2O)_2]_n$, and one copper(I)-thiolate solid **3**, $[Cu(p\text{-}SPhCO_2H)_n]$. This study shows that the reactivity of either the reduced $HSPhCO_2H$ or the oxidized dimeric $(SPhCO_2H)_2$ form of the ligand is ruled by the mild or harsh synthetic conditions in play. Under lower temperature and acidity conditions, the coordination of the carboxylates to Cu(II) and the S−S bond formation/preservation are observed when an *in situ* reduction of Cu(II), cleavage of the S−S bond, and coordination of the thiolates with Cu(I) are happening under harsher conditions of temperature and acidity. Compounds **1** and **2** are polymorphs built up with $\{Cu_2(COO)_4\}$ paddle wheel inorganic units with different dimensionalities: **1** is a 1D structure, and **2** is a 2D network. **3** is a copper-thiolate compound with a lamellar structure of Cu_3S_3 inorganic layers linked through hydrogen bonds between the carboxylic acids. Among those three compounds, the Cu(I)-thiolate solid shows considerably higher chemical and thermal stabilities than the Cu(II)-carboxylates. In addition, **3** exhibits luminescence thermochromism associated with a multiple emission that can be a good potential for temperature sensing.

ASSOCIATED CONTENT

Supporting Information

The Supporting Information is available free of charge on the ACS Publications website at DOI: 10.1021/acs.inorgchem.7b03090.

Experiments and methods, chemicals, syntheses, thermal and chemical stability tests, crystallographic data, PXRD, SEM images, FT-IR, TGA, UV−vis absorption, and emission−excitation spectra (PDF)

Accession Codes

CCDC 1581240−1581241 and 1822344−1822345 contain the supplementary crystallographic data for this paper. These data can be obtained free of charge via www.ccdc.cam.ac.uk/data_request/cif, or by emailing data_request@ccdc.cam.ac.uk, or by contacting The Cambridge Crystallographic Data Centre, 12 Union Road, Cambridge CB2 1EZ, UK; fax: +44 1223 336033.

AUTHOR INFORMATION

Corresponding Authors

*E-mail: alexandra.fateeva@univ-lyon1.fr.

*E-mail: aude.demessence@ircelyon.univ-lyon1.fr.

ORCID

Gilles Ledoux: 0000-0002-0867-1285

Aude Demessence: 0000-0002-8690-5489

Author Contributions

All authors have given approval to the final version of the manuscript.

Notes

The authors declare no competing financial interest.

ACKNOWLEDGMENTS

The authors acknowledge the Synchrotron Soleil for providing access to the crystal beamline (proposal 20150723) and are grateful to Dr. Erik ELKAIM for his assistance with running the experiments. They also thank the CTμ (Centre Technologique des Microstructures of Lyon Univ.) for providing SEM. O.V. thanks the Rhône-Alpes region (ARC 6) for her Ph.D. grant. A.D. thanks the Agence Nationale pour la Recherche for the financial support (FULOR project ANR-13-JS08-0005-01).

REFERENCES

(1) Furukawa, H.; Cordova, K. E.; O'Keeffe, M.; Yaghi, O. M. The Chemistry and Applications of Metal-Organic Frameworks. *Science* **2013**, *341*, 1230444.

(2) Almeida Paz, F. A.; Klinowski, J.; Vilela, S. M. F.; Tomé, J. P. C.; Cavaleiro, J. A. S.; Rocha, J. Ligand design for functional metal−organic frameworks. *Chem. Soc. Rev.* **2012**, *41*, 1088−1110.

(3) Chui, S. S. Y.; Lo, S. M. F.; Charmant, J. P. H.; Orpen, A. G.; Williams, I. D. A chemically functionalizable nanoporous material. *Science* **1999**, *283*, 1148−1150.

(4) Low, J. J.; Benin, A. I.; Jakubczak, P.; Abrahamian, J. F.; Faheem, S. A.; Willis, R. R. Virtual High Throughput Screening Confirmed Experimentally: Porous Coordination Polymer Hydration. *J. Am. Chem. Soc.* **2009**, *131*, 15834−15842.

(5) Veselska, O.; Demessence, A. d^{10} Coinage Metal Organic Chalcogenolates: from Oligomers to Coordination Polymers. *Coord. Chem. Rev.* **2018**, *355*, 240−270.

(6) Baumgartner, M.; Schmalle, H.; Baerlocher, C. Synthesis, Characterization, and Crystal Structure of Three Homoleptic Copper-(I) Thiolates: (Cu(CH3S-))∞, [(C6H5)4P+]2[Cu5(CH3S-)7] · C2H6O2, and [(C3H7)4N+]2[Cu4(CH3S-)6 · CH4O. *J. Solid State Chem.* **1993**, *107*, 63.

(7) Che, C.-M.; Li, C.-H.; Chui, S. S.-Y.; Roy, V. A. L.; Low, K.-H. Homoleptic Copper(I) Arylthiolates as a New Class ofp-T ype Charge Carriers: Structures and Charge Mobility Studies. *Chem. - Eur. J.* **2008**, *14*, 2965−2975.

(8) Yan, H.; Hohman, J. N.; Li, F. H.; Jia, C.; Solis-Ibarra, D.; Wu, B.; Dahl, J. E. P.; Carlson, R. M. K.; Tkachenko, B. A.; Fokin, A. A.; Schreiner, P. R.; Vailionis, A.; Kim, T. R.; Devereaux, T. P.; Shen, Z.-X.; Melosh, N. A. Hybrid metal−organic chalcogenide nanowires with electrically conductive inorganic core through diamondoid-directed assembly. *Nat. Mater.* **2017**, *16*, 349.

(9) Low, K.-H.; Roy, V. A. L.; Chui, S. S.-Y.; Chan, S. L.-F.; Che, C.-M. Highly conducting two-dimensional copper(I) 4-hydroxythiophenolate network. *Chem. Commun.* **2010**, *46*, 7328−7330.

(10) Veselska, O.; Podbevšek, D.; Ledoux, G.; Fateeva, A.; Demessence, A. Intrinsic Triple-Emitting 2D Copper Thiolate Coordination Polymer as a Ratiometric Thermometer Working over 400 K Range. *Chem. Commun.* **2017**, *53*, 12225−12228.

(11) Huang, X.; Sheng, P.; Tu, Z.; Zhang, F.; Wang, J.; Geng, H.; Zou, Y.; Di, C.-a.; Yi, Y.; Sun, Y.; Xu, W.; Zhu, D. A two-dimensional p−d conjugated coordination polymer with extremely high electrical conductivity and ambipolar transport behaviour. *Nat. Commun.* **2015**, *6*, 7408.

(12) (a) Zhang, Y.-N.; Wang, Y.-Y.; Hou, L.; Liu, P.; Liu, J.-Q.; Shi, Q.-Z. A series of metal−organic coordination polymers assembled with

DOI: 10.1021/acs.inorgchem.7b03090
Inorg. Chem. XXXX, XXX, XXX−XXX

disulfide ligand involving in situ cleavage of S−S under co-ligand intervention. *CrystEngComm* **2010**, *12*, 3840−3851. (b) Zhang, Y.-N.; Liu, P.; Wang, Y.-Y.; Wu, L.-Y.; Pang, L.-Y.; Shi, Q.-Z. Syntheses and Crystal Structures of a Series of Zn(II)/Cd(II) Coordination Polymers Constructed from a Flexible 6,6′-Dithiodinicotinic Acid. *Cryst. Growth Des.* **2011**, *11*, 1531−1541. (c) Zhang, Y.-N.; Wang, Y.-Y.; Yang, G.-P.; Hou, L.; Shi, Q.-Z. Syntheses, structures, and properties of lanthanide−organic frameworks with flexible disulfide derivative of carboxylate. *Inorg. Chim. Acta* **2010**, *363*, 3413−3419. (d) Tseng, T.-W.; Luo, T.-T.; Shih, Y.-R.; Shen, J.-W.; Lee, L.-W.; Chiang, M.-H.; Lu, K.-L. Self-triggered conformations of disulfide ensembles in coordination polymers with multiple metal clusters. *CrystEngComm* **2015**, *17*, 2847. (e) De la Pinta, N.; Fidalgo, L.; Madariaga, G.; Lezama, L.; Cortés, R. Guest Driven Structural Correlations in DPDS [Di(4-pyridyl)disulfide]-Based Coordination Polymers. *Cryst. Growth Des.* **2012**, *12*, 5069−5078. (f) Chen, X.-L.; Qiao, Y.-L.; Gao, L.-J.; Cui, H.-L.; Zhang, M.-L.; Lv, J.-F.; Hou, X.-Y. Synthesis, Structure, and Characterization of Two Zn/Cd Coordination Polymers with Flexible Disulfide Carboxylate Derivatives. *Z. Anorg. Allg. Chem.* **2013**, *639*, 403−408. (g) De la Pinta, N.; Madariaga, G.; Ezpeleta, T.; Fidalgo, M. L.; Lezama, L.; Cortés, E. Spin canting in the $[Co_2(NCO)_4(DPDS)_4]\cdot 3H_2O$ [DPDS = di(4-pyridyl)disulfide] coordination polymer. *Polyhedron* **2013**, *52*, 1256−1261. (h) Kondo, M.; Shimamura, M.; Noro, S.; Kimura, Y.; Uemura, K.; Kitagawa, S. Synthesis and Structures of Coordination Polymers with 4,4@-Dipyridyldisulfide. *J. Solid State Chem.* **2000**, *152*, 113−119.

(13) (a) Liu, G.-N.; Li, K.; Fan, Q.-S.; Sun, H.; Li, X.-Y.; Han, X.-N.; Li, Y.; Zhang, Z.-W.; Li, C. A simultaneous disulfide bond cleavage, N,S-bialkylation/N-protonation and self-assembly reaction: syntheses, structures and properties of two hybrid iodoargentates with thiazolyl-based heterocycles. *Dalton Trans.* **2016**, *45*, 19062. (b) Zhu, H.-B.; Wu, Y.-F.; Zhao, Y.; Hu, J. Unprecedented metal-mediated in situ reactions of heterocyclic disulfide of di[4-(pyridin-2-yl)-pyrimidinyl]-disulfide. *Dalton Trans.* **2014**, *43*, 17156. (c) Zhu, Q.; Shang, T.; Tan, C.; Hu, S.; Fu, R.; Wu, X. Formation of Zn(II) and Cd(II) Coordination Polymers Assembled by Triazine-Based Polycarboxylate and in-Situ-Generated Pyridine-4-thiolate or Dipyridylsulfide Ligands: Observation of an Unusual Luminescence Thermochromism. *Inorg. Chem.* **2011**, *50*, 7618−7624. (d) Fang, S.-M.; Chen, M.; Yang, X.-G.; Hu, J.-Y.; Liu, C.-S. Construction of metal−organic replica of sqc1121 network based on a multifunctional ligand via solvothermal in situ disulfide cleavage reaction. *Inorg. Chem. Commun.* **2012**, *22*, 101−103. (e) Chen, H.-R. Synthesis, Structure and Physical Properties of A Novel 2D Cd(II) Coordination Polymer Involving 4-Thiopyridine Based on in situ Formation from 4,4′-Dithiodipyridine. *Bull. Korean Chem. Soc.* **2014**, *35*, 2839. (f) Zhu, H.-B.; Gou, S.-H. In situ construction of metal−organic sulfur-containing heterocycle frameworks. *Coord. Chem. Rev.* **2011**, *255*, 318−338. (g) Han, L.; Bu, X.; Zhang, Q.; Feng, P. Solvothermal in Situ Ligand Synthesis through Disulfide Cleavage: 3D (3,4)-Connected and 2D Square-Grid-Type Coordination Polymers. *Inorg. Chem.* **2006**, *45*, 5736−5738.

(14) (a) Xie, Y.; He, J.; Wang, T.; Zeng, H. Syntheses, structures, and luminescence of two Zn(II) coordination polymers based on 5-(4-imidazol-1-ylphenyl)-2H-tetrazole and carboxylates. *J. Coord. Chem.* **2015**, *68*, 1733. (b) Ge, S.-Z.; Liu, Q.; Deng, S.; Sun, Y.-Q.; Chen, Y.-P. Two New Luminescent Cadmium Thiolato-carboxylates with 2,20-Bipyridine. *J. Inorg. Organomet. Polym. Mater.* **2013**, *23*, 571−578. (c) Rowland, C. E.; Belai, N.; Knope, K. E.; Cahill, C. L. Hydrothermal Synthesis of Disulfide-Containing Uranyl Compounds: In Situ Ligand Synthesis versus Direct Assembly. *Cryst. Growth Des.* **2010**, *10*, 1390−1398.

(15) Turbeville, W.; Yap, N. The chemistry of copper-containing sulfur adsorbents in the presence of mercaptans. *Catal. Today* **2006**, *116*, 519.

(16) Esmieu, C.; Orio, M.; Le Pape, L.; Lebrun, C.; Pécaut, J.; Ménage, S.; Torelli, S. Redox-Innocent Metal-Assisted Cleavage of S−S Bond in a Disulfide-Containing Ligand. *Inorg. Chem.* **2016**, *55*, 6208−6217.

(17) Yam, V. W.-W.; Au, V. K.-M.; Leung, S. Y.-L. Light-Emitting Self-Assembled Materials Based on d^8 and d^{10} Transition Metal Complexes. *Chem. Rev.* **2015**, *115*, 7589−7728.

(18) (a) Benito, Q.; Maurin, I.; Cheisson, T.; Nocton, G.; Fargues, A.; Garcia, A.; Martineau, C.; Gacoin, T.; Boilot, J.-P.; Perruchas, S. Mechanochromic Luminescence of Copper Iodide Clusters. *Chem. - Eur. J.* **2015**, *21*, 5892. (b) Tard, C.; Perruchas, S.; Maron, S.; Le Goff, X. F.; Guillen, F.; Garcia, A.; Vigneron, J.; Etcheberry, A.; Gacoin, T.; Boilot, J.-P. Thermochromic Luminescence of Sol-Gel Films Based on Copper Iodide Clusters. *Chem. Mater.* **2008**, *20*, 7010−7016.

(19) Troyano, J.; Perles, J.; Amo-Ochoa, P.; Martinez, J. I.; Gimeno, M. C.; Fernandez-Moreira, V.; Zamora, F.; Delgado, S. Luminescent Thermochromism of 2D Coordination Polymers Based on Copper(I) Halides with 4-Hydroxythiophenol. *Chem. - Eur. J.* **2016**, *22*, 18027−18035.

(20) Veselska, O.; Okhrimenko, L.; Guillou, N.; Podbevsek, D.; Ledoux, G.; Dujardin, C.; Monge, M.; Chevrier, D. M.; Yang, R.; Zhang, P.; Fateeva, A.; Demessence, A. Intrinsic Dual-Emitting Gold Thiolate Coordination Polymer, $[Au(+I)(p\text{-}SPhCO_2H)]_n$, for Ratiometric Temperature Sensing. *J. Mater. Chem. C* **2017**, *5*, 9843.

(21) Gautier, R.; Latouche, C.; Paris, M.; Massuyeau, F. Thermochromic Luminescent Materials and Multi-Emission Bands in d^{10} Clusters. *Sci. Rep.* **2017**, *7*, 45537.

DOI: 10.1021/acs.inorgchem.7b03090
Inorg. Chem. XXXX, XXX, XXX−XXX